Adsorption and Electrode Reactions of Disulfonated Anthraquinones at Mercury Electrodes

Peixin He, Richard M. Crooks, and Larry R. Faulkner*

Department of Chemistry, University of Illinois, Urbana, Illinois 61801 *(Received: June 19, 1989)*

Three sulfonated compounds were examined: 2,6-anthraquinonedisulfonate, sodium salt (2,6-AQDS); 1,5-anthraquinonedisulfonate, sodium salt (1,5-AQDS); and 2-anthraquinonemonosulfonate, sodium salt (2-AQMS). Extensive studies of 2,6-AQDS were carried out. This compound undergoes reversible charge exchange with the electrode in an adsorbed state. Electrocapillary curves show that desorption occurs near −0.8 V vs Ag/AgCl, KCl (1 M). Chronocoulometry and cyclic voltammetry were used to evaluate surface coverage vs the concentration of 2,6-AQDS in 0.1 M HNO_3. Over the range from 2.5×10^{-8} to 5×10^{-5} M the surface excess obeys a Langmuir isotherm with a saturation limit of 0.94×10^{-10} mol/cm^2, corresponding to 180 Å^2/molecule. Under all conditions, the adsorbed couple shows a standard potential more positive than that for the couple involving dissolved species; hence, the reduced form is the more strongly adsorbed. Effects of pH were examined extensively. Both couples (adsorbed and dissolved) show a negative shift in formal potential of nearly 60 mV/pH unit in the pH range below 8; hence, the reactions involve one proton per electron, as expected. The formal potentials become independent of pH at pH > 11. In solutions with 2,6-AQDS concentrations above 2×10^{-5} M an extremely sharp, reversible pair of spikes develops in the cyclic voltammetry for the adsorbed couple. The spikes are not seen for 1,5-AQDS, but other aspects of behavior for 1,5-AQDS are similar to those of 2,6-AQDS. The origin of the spikes is discussed via a model involving hydrogen-bonded aggregates. Extensive exposure of a mercury surface to high concentrations of 2,6-AQDS produces a catalytic effect on the electrode reaction involving the dissolved quinone. Further exposure causes an inhibition of the same process. These effects are attributed to the growth of extended films on the mercury.

Introduction

In this paper, we provide a detailed description of the electrochemical behavior of 2,6-anthraquinonedisulfonate (2,6-AQDS, Figure 1) at mercury surfaces in contact with aqueous electrolytes. In less detail, we also discuss the behavior of 1,5-anthraquinonedisulfonate (1,5-AQDS) and 2-anthraquinonemonosulfonate (2-AQMS). We will show that the anthraquinonedisulfonates, particularly 2,6-AQDS, exhibit a wide range of phenomena of interest to contemporary electrochemistry. For example, they form extremely tightly bound adsorbate layers, which are stable in both redox forms. Under accessible, convenient conditions, these layers can be interconverted between redox forms with virtually ideal electrochemical responses. Thus, they are excellent model systems for fresh studies of interfacial dynamics. Under other conditions, adsorbed 2,6-AQDS shows extremely sharp spikes in its voltammetry, apparently reflecting extensive reorganization, probably a phase transition in the adlayer, based on strong intermolecular interactions. In these circumstances, the layers can prove useful as models for studies of structural alterations in two-dimensional assemblies. We also highlight some autocatalytic and autoinhibitory effects of these films on the electrode kinetics of the dissolved quinones.

The electrochemical reactions of the monosulfonate, 2-AQMS, have been examined previously in some detail, but in a restricted pH range. Gill and Stonehill[1] and Furman and Stone[2] showed that 2-AQMS produces a well-developed polarographic wave in basic media. Their results were concordant with a two-electron, one-proton reduction to produce the singly deprotonated dihydroxyanthracene

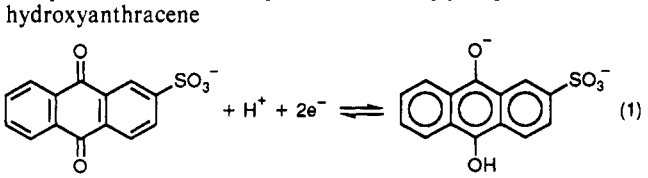

(1)

Anson and Epstein[3] later noticed that the cyclic voltammetry of 2-AQMS showed an unusually sharp reduction peak, which they confirmed as being due to the adsorption of the quinone at mercury. They carried out extensive chronocoulometric investigations, all at pH 8.9, in which they varied the concentrations of competitively adsorbing anions.

The disulfonated anthraquinones have also evoked interest, but the properties discussed in this paper have not been delineated. Furman and Stone[1] seem to have produced the first electrochemical studies. They noted unusual wave slopes in polarography. Similar work was done by Berg,[4] whose figures clearly show adsorption effects for 1-AQMS and 1,5-AQDS in pH 7 phosphate buffer with 1% ethanol. Berg[5] later studied 1,5-AQDS and 2,6-AQDS by cyclic voltammetry at mercury and saw irreversibility in the behavior for 1,5-AQDS, but not for 2,6-AQDS, at pH 7. The clear recognition of adsorption in systems involving disulfonated anthraquinones came in the work by Ferenc et al.,[6] Palyi and Peter,[7] and Savenko and co-workers.[8,9] These papers are chiefly aimed at explanations of pre- and postwaves in the polarography of unbuffered, pH 7 solutions. More recently, Soriaga and Hubbard[10] examined the adsorption of 2,6-AQDS and 1,5-AQDS on Pt by thin-layer coulometry and indicated that both were adsorbed from 1 M $HClO_4$ at densities corresponding to monolayers of molecules situated flat against the electrode. Hubbard's group later characterized the effects of concentration and temperature and the effect of exposure to iodide on the adsorption.[11-17] Wipf et al.[18] examined 2-AQMS and 2,6-AQDS

* To whom correspondence should be addressed.

(1) Gill, R.; Stonehill, H. I. *J. Chem. Soc.* **1952**, 1845.
(2) Furman, N. H.; Stone, K. G. *J. Am. Chem. Soc.* **1948**, *70*, 3055.
(3) Anson, F. C.; Epstein, B. *J. Electrochem. Soc.* **1968**, *115*, 1155.
(4) Berg, H. *Chem. Tech. (Berlin)* **1954**, *6*, 585.
(5) Berg, H. *Naturwissenschaften* **1961** *48*, 714.
(6) Ferenc, P.; Palyi, G.; Szabados, I. *Magy. Kem. Foly.* **1961**, *67*, 428.
(7) Palyi, G.; Peter, F. *Chem. Zvesti* **1962**, *16*, 354.
(8) Savenko, E. M.; Liebman, D. S.; Tedoradze, G. A. *Elektrokhimiya* **1978**, *14*, 477.
(9) Savenko, E.; Tedoradze, G. *Collect. Czech. Chem. Commun.* **1983**, *48*, 550.
(10) Soriaga, M. P.; Hubbard, A. T. *J. Am. Chem. Soc.* **1982**, *104*, 2735.
(11) Soriaga, M. P.; Hubbard, A. T. *J. Am. Chem. Soc.* **1982**, *104*, 2742.
(12) Soriaga, M. P.; Hubbard, A. T. *J. Am. Chem. Soc.* **1982**, *104*, 3937.
(13) Soriaga, M. P.; Wilson, P. H.; Hubbard, A. T.; Benton, C. S. *J. Electroanal. Chem.* **1982**, *142*, 317.
(14) Soriaga, M. P.; Stickney, J. L.; Hubbard, A. T. *J. Electroanal. Chem.* **1983**, *144*, 207.
(15) Soriaga, M. P.; White, J. H.; Hubbard, A. T. *J. Phys. Chem.* **1983**, *87*, 3048.
(16) Hubbard, A. T.; Stickney, J. L.; Soriaga, M. P.; Chia, V. K. F.; Rosasco, S. D.; Schardt, B. C.; Solomon, T.; Song, D.; White, J. H.; Wieckowski, A. *J. Electroanal. Chem.* **1984**, *168*, 43.

0022-3654/90/2094-1135$02.50/0

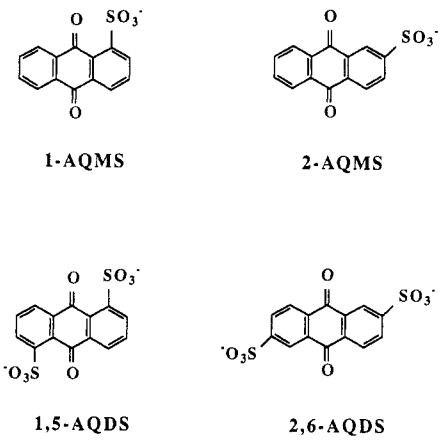

Figure 1. Structures of compounds investigated in this study.

in strongly basic solutions of water and alcohols at mercury ultramicroelectrodes. Their aim was to quantify the homogeneous disproportionation of the quinone radical anion intermediates. They worked at pH values above the pK_a for the second phenolic proton on the dihydroxyanthracene, so that the ultimate reduction product of each quinone was the fully deprotonated species, e.g.

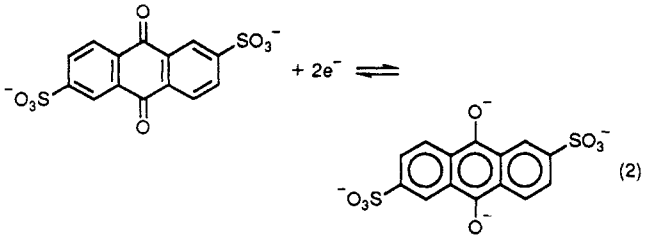

In this paper, we consider mainly behavior in acidic media where the expected electrode process is the two-electron, two-proton conversion of the quinone to the dihydroxyanthracene

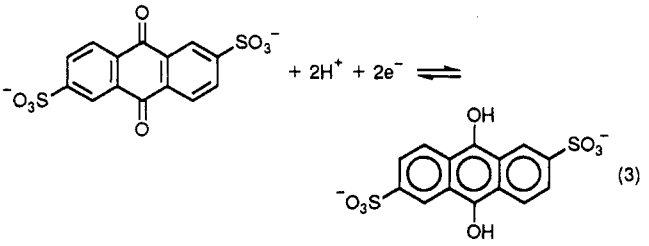

A few of our observations were presented earlier[19] as illustrations of the capabilities of some new instrumentation. This detailed report is offered in the expectation that others will find these systems useful for fundamental investigations of electrochemical dynamics.

Experimental Section

Anthraquinone-2,6-disulfonic acid, disodium salt (2,6-AQDS), anthraquinone-1,5-disulfonic acid, disodium salt (1,5-AQDS), and anthraquinone-2-sulfonic acid, sodium salt (2-AQMS), were obtained from Aldrich Chemical Co. All were recrystallized from water 1–2 times with decolorizing charcoal. The process was performed in the dark due to photochemical reactions which turned the crystals off-color. In their purified state the 2-AQMS and 1,5-AQDS are yellow powders, and the 2,6-AQDS is a cream-colored powder.

Buffer solutions were made from analytical reagents. To obtain different buffer solutions for pH 1–13, HNO_3, HOAc–KOAc, NaH_2PO_4–NaOH, H_3BO_3–NaOH, Na_2HPO_4–NaOH, and NaOH were used, with the dominant component always at 0.01 M or higher. If necessary, KNO_3 was used to supplement the ionic strength to a constant value of 0.1 M.

Water was purified by a Milli-Q filtering system (Millipore). Mercury was obtained from Bethlehem Instruments and was triply distilled by the manufacturer.

A custom-built cybernetic potentiostat[19] was used for all experiments. This instrument was the prototype for the commercial Bioanalytical Systems BAS-100 electrochemical analyzer. The EG&G PARC Model 303 static mercury drop electrode (SMDE) was used with an Ag/AgCl, KCl (1 M) reference. All potentials are reported with respect to this reference.

A three-compartment cell was used for coulometric bulk electrolysis. The working electrode was a large-area mercury pool, which was in a sample compartment together with an Ag/AgCl, KCl (1 M) reference electrode. A Pt foil counter electrode was installed in another compartment, which was separated from the working compartment by a third compartment that joined the others via two fritted glass junctions. A solution of 0.1 M HNO_3 was used as an electrolyte.

In most cyclic voltammetric and chronocoulometric work, a precise delay time (normally 5 s) was allowed, after connecting the cell and expressing the hanging mercury drop, before the scan or step sequence was initiated. This was done in order to establish a given extent of adsorption. The effects of variation in this "quiet time" are discussed below.

All solutions were degassed prior to experiments by bubbling nitrogen through them. During the course of each experiment, a blanket of nitrogen was maintained over the solution.

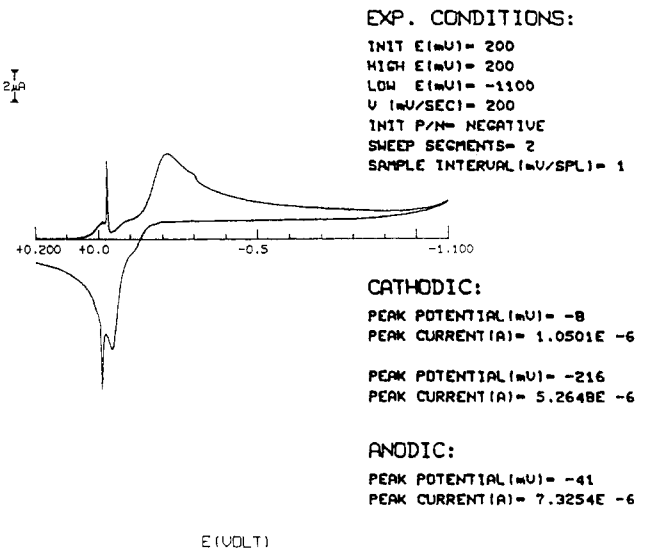

Figure 2. Cyclic voltammogram of 1×10^{-3} M 2,6-AQDS in 0.1 M HNO_3.

Results and Discussion

Overview of Behavior. Most of the work was done on 2,6-AQDS. The behavior of 1,5-AQDS and 2-AQMS was studied only as a supplement and comparison, as necessary.

A cyclic voltammogram of 1 mM 2,6-AQDS in 0.1 M HNO_3 is shown in Figure 2. On the negative scan, the prominent peak at −0.2 V is due to the reduction of 2,6-AQDS diffusing from the bulk solution. Near 0.0 V, a small peak with an extremely narrow superimposed spike (only a few millivolts wide) is seen. Between the spike and the diffusion peak, at −0.1 V, there is another small wave. All of the oxidation peaks overlap on the positive scan, where a spike is also seen. The redox process related to the diffusion peak is a quasireversible reaction, giving a peak separation (cathodic vs anodic) of 150 mV at 100 mV/s scan rate.

The cathodic prepeak at 0.0 V originates from a surface-bound species. The relative heights of the peaks at 0.0 and −0.2 V change with the scan rate, with the prepeak becoming dominant at high scan rate, as one expects for assignment to surface and diffusion waves, respectively.[20] If the bulk concentration is reduced to 1×10^{-5} M, the diffusion peak at −0.2 V and the cathodic spike

(17) Soriaga, M. P.; Binamira-Soriaga, E.; Hubbard, A. T.; Benziger, J. B.; Pang, K.-W. P. *Inorg. Chem.* **1985**, *24*, 65.
(18) Wipf, D. O.; Wehmeyer, K. R.; Wightman, R. M. *J. Org. Chem.* **1986**, *51*, 4760.
(19) He, P.; Avery, J. P.; Faulkner, L. R. *Anal. Chem.* **1982**, *54*, 1313A.

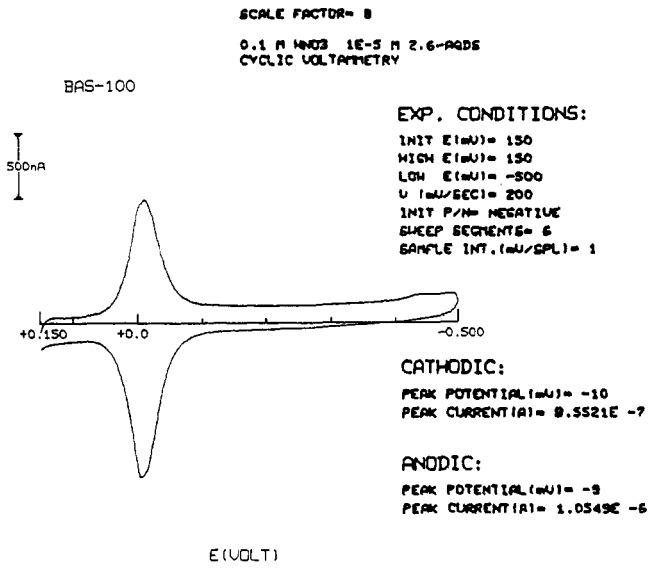

Figure 3. Cyclic voltammogram of 1×10^{-5} M 2,6-AQDS in 0.1 M HNO_3.

vanish, but a pair of surface peaks is still there, as shown in Figure 3. These peaks are symmetric; their separation is close to zero; the peak heights are proportional to the scan rate; and their symmetry does not vary at high scan rate. These are strong evidences for adsorption of a species that undergoes a reversible electrochemical reaction in the adsorbed state.[20-22]

By controlled potential bulk electrolysis at −0.8 V, we confirmed that the reductions of all three sulfonated anthraquinones are two-electron processes. These electrolyses were terminated when the current fell below 1% of the initial current. The current at the cutoff was considered as a constant background, for which the accumulated charge was corrected. The n values computed from the resulting net charges were 1.79 ± 0.01, 1.93 ± 0.02, and 1.91 ± 0.01 for 2,6-AQDS, 1,5-AQDS, and 2-AQMS, respectively. The fact that all values lie below 2.00 is possibly due to an early cutoff or inaccurate correction for background charge.

For an ideal reversible adsorption peak, the electron-transfer number n can be obtained from the peak width at half-height, which is $90.6/n$ mV.[21,22] The width observed here is 48 mV for the reduction peak and 45.6 mV for the oxidation peak. With all other aspects of the peak being nearly ideal, these values suggest that two electrons are involved in the redox couple for the adsorbates, just as for the dissolved species. The clearly reversible electrochemistry for the adsorbate is in sharp contrast with the behavior found by Soriaga and Hubbard[10] for 2,6-AQDS adsorbed on Pt. There, the quinone/hydroquinone transformation did not occur. The difference in behavior on Pt and Hg is probably due to very substantial differences in surface bonding.[17]

The potential range of adsorption of 2,6-AQDS on the mercury electrode was observed by recording the electrocapillary curves, an example of which is shown in Figure 4. Adsorbed species obviously exist at all potentials more positive than −0.8 V. Taking Figures 2–4 together, it is clear that oxidized 2,6-AQDS is surface-bound at potentials more positive than 0.0 V and that the reduced form is surface-bound between 0.0 and −0.8 V. Beyond −0.8 V the reduced form desorbs and exists only in solution. The positive location of the adsorption peaks with respect to the diffusive peaks implies that the reduced form of 2,6-AQDS is more strongly adsorbed than the oxidized form.[20-22]

The shape of the electrocapillary curve is noteworthy. Since the surface excess charge is proportional to the slope, the inflection between 0.0 and −0.3 V indicates a dramatic change of excess charge on the surface of the electrode: from a positive value, to

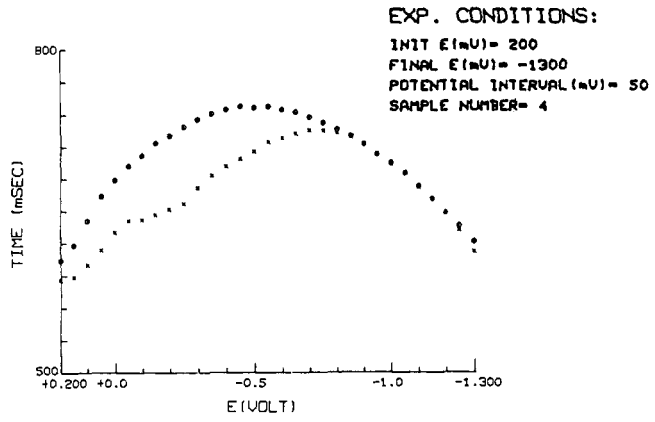

Figure 4. Electrocapillary curves obtained in 0.1 M HNO_3 solution: (○) no 2,6-AQDS, (×) 1×10^{-3} M 2,6-AQDS.

almost zero, then again to a positive value. This feature may be important in understanding the origin of the spike in the cyclic voltammogram, as will be discussed later.

The amount of adsorbate was determined by double-step chronocoulometry[22-24] between +0.2 and −1.0 V. Since no adsorption occurs at the potential of the forward step, as known from the electrocapillary curve, the difference in the intercepts for the forward and reverse Anson plots provided the initial surface excess (assuming $n = 2$). The surface excess was obtained independently from the area of the cathodic surface peak in the cyclic voltammogram. In both cases, the charge obtained for 2,6-AQDS concentrations at or above 5×10^{-5} M was $(1.50–1.68) \times 10^{-5}$ C/cm^2, which is equivalent to a maximum surface excess of $(0.78–0.87) \times 10^{-10}$ mol/cm^2 at +0.2 V. This range seems to be a little less than the maximum possible monolayer adsorption with a flat orientation of 2,6-AQDS on the surface of the mercury. Moreover, it is only about half the largest surface excess found by Anson and Epstein for 2-AQMS. Our data correspond to 190–210 Å^2/molecule, whereas Soriaga and Hubbard's work[10] indicates that 2,6-AQDS in a flat orientation occupies about 130 Å^2/molecule. The adsorption peak area for oxidation is normally a little larger than the one for reduction; thus, the reduced form may develop a more compact adsorbed layer.

The time needed to establish adsorption equilibrium is dependent on the bulk concentration.[21,22] We found experimentally that the intercept difference in chronocoulometry for 2,6-AQDS at 2×10^{-5} M did not change appreciably (±2%) with quiet time, as long as that period was 2 s or longer. For shorter quiet times, the expected rise in coverage with increasing quiet time was observed. These results suggest that our standard delay of 5 s is sufficient to establish equilibrium at these concentrations and above. Longer equilibrium times would be needed for lower concentrations.

The equilibrium surface coverage is a function of the bulk concentration. A limiting coverage is attained when the bulk concentration is higher than a few times 10^{-5} M, as discussed above. To define the adsorption isotherm for lower concentrations, the coverages at equilibrium were obtained by integrating cyclic voltammetric peaks for different bulk concentrations. Equilibrium was checked by periodically scanning the potential at 50 mV/s from +0.2 to −0.2 V, until the adsorption peak did not increase with time. Ten cycles were generally sufficient. We were able to obtain readily integrable adsorption peaks for 2,6-AQDS concentrations as low as 2.5×10^{-8} M. The relationship between the surface coverage and bulk concentration is shown in Figure 5. The shape of the curve is reminiscent of a Langmuir isotherm[21,22]

$$\frac{\Gamma_i}{\Gamma_{i,s} - \Gamma_i} = b_i c_i \qquad (4)$$

(20) Wopschall, R. H.; Shain, I. *Anal. Chem.* **1967**, *39*, 1514.
(21) Laviron, E. *Electroanal. Chem.* **1982**, *12*, 53.
(22) Bard, A. J.; Faulkner, L. R. *Electrochemical Methods*; Wiley: New York, 1980.
(23) Anson, F. C. *Anal. Chem.* **1966**, *38*, 54.
(24) Christie, J. H.; Osteryoung, R. A.; Anson, F. C. *J. Electroanal. Chem.* **1967**, *13*, 236.

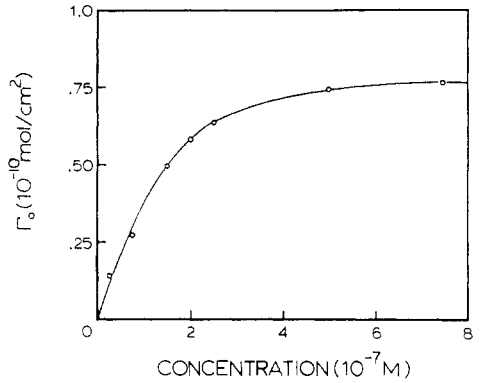

Figure 5. Relationship between the surface excess of 2,6-AQDS and bulk concentration in 0.1 M HNO_3.

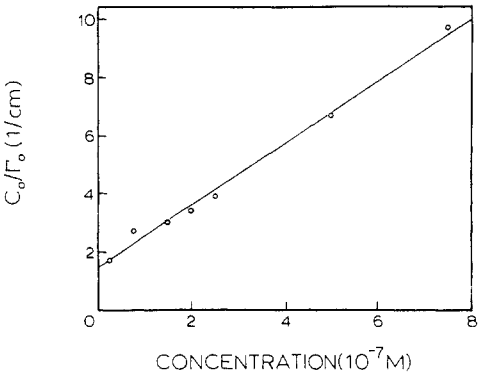

Figure 6. Linear plot of the data in Figure 5.

where Γ_i is the surface excess of an adsorbed species i, $\Gamma_{i,s}$ is the surface excess at maximum coverage, b_i is the adsorption coefficient, and c_i is the bulk concentration. Equation 4 can be linearized in the form

$$\frac{c_i}{\Gamma_i} = \frac{1}{\Gamma_{i,s} b_i} + \frac{c_i}{\Gamma_{i,s}} \tag{5}$$

For c_i/Γ_i plotted versus c_i, a straight line is predicted. Our data adhere to this prediction, as shown in Figure 6. From the least-squares slope, the maximum surface coverage of the oxidized form $\Gamma_{O,s}$ is found to be 0.94×10^{-10} mol/cm^2, which is a little higher than the limiting measured value given earlier and corresponds to about 180 Å^2/molecule. The adsorption coefficient of the oxidized form b_O is 7.1×10^6 M^{-1}.

According to Laviron,[21,25,26] the location of a prewave or postwave on the potential axis is not only due to the difference of the relative adsorption strength of reactant and product but also to the interactions between the adsorbed molecules. The separation between the adsorption peak potential $E_{p,ad}$ and the formal potential $E^{\circ\prime}$, for the couple involving both species in solution can be expressed by

$$E_{p,ad} - E^{\circ\prime} = \frac{RT}{nF} \ln \frac{b_R}{b_O} + \frac{RT}{nF}(a_R - a_O)\nu\theta_T \tag{6}$$

where a_R and a_O are the constants of interaction between molecules of R and molecules of O, respectively. The parameter ν is the number of water molecules displaced by one molecule of O or R, and θ_T is the total coverage. On the right side, the first term represents the relative adsorption strength of reduced and oxidized forms. The second term represents the interaction between the adsorbed molecules.

For 2,6-AQDS, the adsorption peak shape, half peak width, and peak potential do not change with the surface coverage, as long as the surface is not saturated. These are strong evidences that the adsorption of oxidized 2,6-AQDS follows a true Langmuir isotherm, in which no interaction exists between molecules. The second term on the right side of eq 6 would then be zero. The ratio b_R/b_O could be readily evaluated if $E^{\circ\prime}$ for the couple involving dissolved species can be defined. This is not straightforward, since the cathodic diffusion wave is shifted by obvious quasireversibility, and the anodic diffusion wave is entangled with the anodic surface wave. The results in Figure 13 and extrapolations of pH dependences (both discussed later) indicate that $E^{\circ\prime}$ for the solution couple is between −0.090 and −0.100 V in 0.1 M HNO_3. With the cathodic surface wave at −0.010 V, one calculates b_R/b_O = 500–1000. Thus b_R is (3–7) $\times 10^9$ M^{-1}.

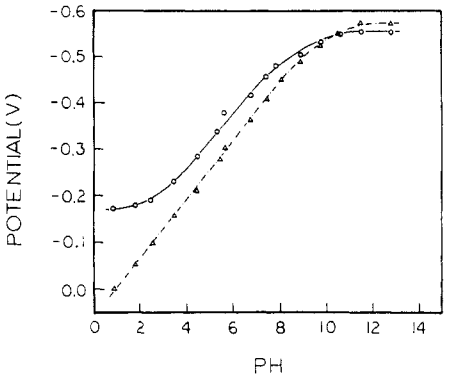

Figure 7. Relationship between peak potentials and solution pH values: (○) diffusion peak, (△) adsorption peak.

pH Effects. The electrochemical reactions of 2,6-AQDS involve protons. Both the adsorption peak and the diffusion peak are shifted negatively as the pH is made higher, as shown in Figure 7. Since the adsorption peak overlaps the diffusion peak at high pH, a low bulk concentration was used to observe the behavior of the adsorption peak. The peak potentials shift linearly with pH below 7. In this range, the slope for the diffusion peak is 57 mV/pH unit, indicating that each electron transferred is matched by one proton. The slope for the adsorption peak is 63 mV/pH unit. In this case, the shift of the peak potential not only is due to the proton dependence of the redox reaction involving adsorbed species but also reflects any change in adsorption strength of the reduced form relative to that of the oxidized form with pH. The faster peak potential shift toward the negative direction for the adsorbed redox couple suggests that the relative adsorption strength of the reduced form decreases as pH increases. For the diffusion peak, the slope of peak potential vs pH is much smaller at pH values below 3, possibly because of the irreversibility of the electrochemical reaction at low pH.

The pK_a values for the two phenolic protons in reduced 2,6-AQDS are expected[5,27] to be near 7.35 and 10.3; thus, one ought to see a slope change from 59 mV/pH unit to 29 mV/pH unit at pH 7.35 and then a further change to zero slope above pH 10.3. These expectations are borne out in Figure 7; thus, the electrode reaction for dissolved species is confirmed as eq 3 for pH below 7, eq 2 for pH above 11, and the analogue to eq 1 for pH between 7 and 11. The plot for the adsorption peak in Figure 7 does not roll over as rapidly as that for the diffusive peak, but it does become flat at pH values above 11. Apparently, the first pK_a for loss of a phenolic proton from the adsorbed reduced form is somewhat higher than for the dissolved species. A value between 9 and 10 would account for our curve.

At high pH, the adsorption peak overlaps with the diffusion peak, but the adsorption still exists. This can be seen from the intercept difference in chronocoulometry or from the cyclic voltammogram when the 2,6-AQDS concentration is low. The extent of maximum absorption shows little change over the pH range 1–13. The pseudocapacitance peak in the ac polarogram, originating from the rapid change in surface coverage at the

(25) Laviron, E. *J. Electroanal. Chem.* **1974**, *52*, 395.
(26) Laviron, E. *J. Electroanal. Chem.* **1975**, *63*, 245.
(27) Ksenzhek, O. S.; Petrova, S. A.; Oleinik, S. V.; Kokodyashnyi, M. V.; Moskovskii, V. Z. *Elektrokhimiya* **1977**, *13*, 182.

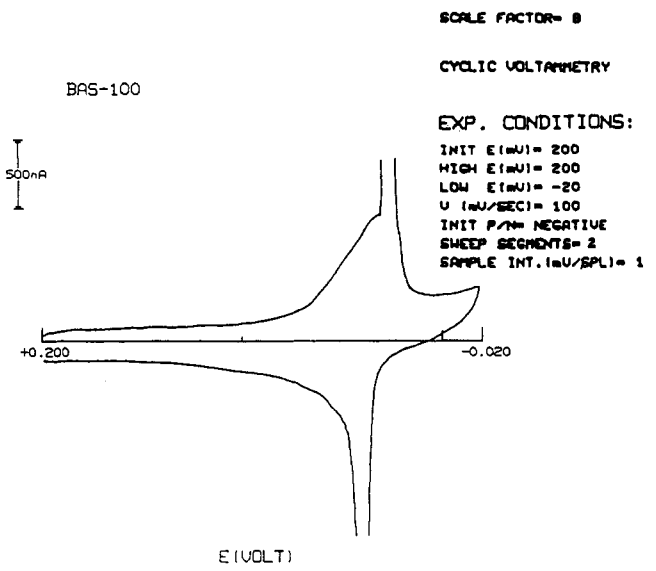

Figure 8. A closer view of the spike. 1×10^{-3} M 2,6-AQDS in 0.1 M HNO_3.

potential of desorption, remains at −0.75 V as the solution pH changes from 1 to 7.5; hence, the desorption potential does not change with pH.

The reversibility of the 2,6-AQDS couple involving diffusing species becomes better as the pH rises. At pH = 9, the peak separation is 53 mV, and the peak heights are maximal. At high pH, the peak separation enlarges again.

Origin of the Spike. As shown in Figure 2, on both negative and positive potential scans, unusually sharp and narrow spikes are seen for 2,6-AQDS. Four characteristics of the spike are noteworthy: (a) The spike is only a few millivolts wide and accompanies the surface waves. (b) The spike appears only when full coverage of the electrode surface is approached. (c) Its height increases with the bulk concentration, but not linearly. (d) The spike is also pH dependent; it vanishes as the pH is taken higher.

It is apparent that the spike arises from some sort of surface phenomenon, since it is much too narrow to result from any diffusion process.[21,28] According to Lippmann's equation,[22] the differential capacitance of the double layer is equal to the second derivative of the interfacial tension with respect to potential. If the second derivative of the electrocapillary curve in Figure 4 is taken, a "capacitance" peak indeed appears at the spike potential. The current spike occurs partly because it is needed to charge this peak capacitance. However, some of the characteristics of the spike suggest a faradaic phenomenon that produces a pseudocapacitance.

It is often true that reorganization of adsorbed species causes changes in the double-layer charge. Since the surface excess charge changes unusually at the potential where the spike happens, it is plausible that the surface-bound 2,6-AQDS undergoes some sort of rearrangement. If this process stabilizes the reduced form, the activity of the reduced form will be decreased. Since the redox reaction of adsorbed 2,6-AQDS is reversible, the surface activity ratio of the reduced and oxidized forms will be concordant with the Nernst equation. Due to the reorganizationally induced decrease in the activity of the reduced form, the oxidized form must be suddenly further reduced. If the newly formed reduced form is further stabilized, the process will propagate, and a faradaic current spike is thus developed. Laviron has discussed such ideas in detail.[21] Figure 8 shows a closer view of the spike. The reduction current drops to a very low level after spike. This indicates the rapid full consumption of the oxidized surface-bound 2,6-AQDS within the spike, as one would predict from the mechanism just discussed.

A similar conclusion can be drawn from the ac voltammogram shown in Figure 9A. A sudden drop of ac current is seen at the

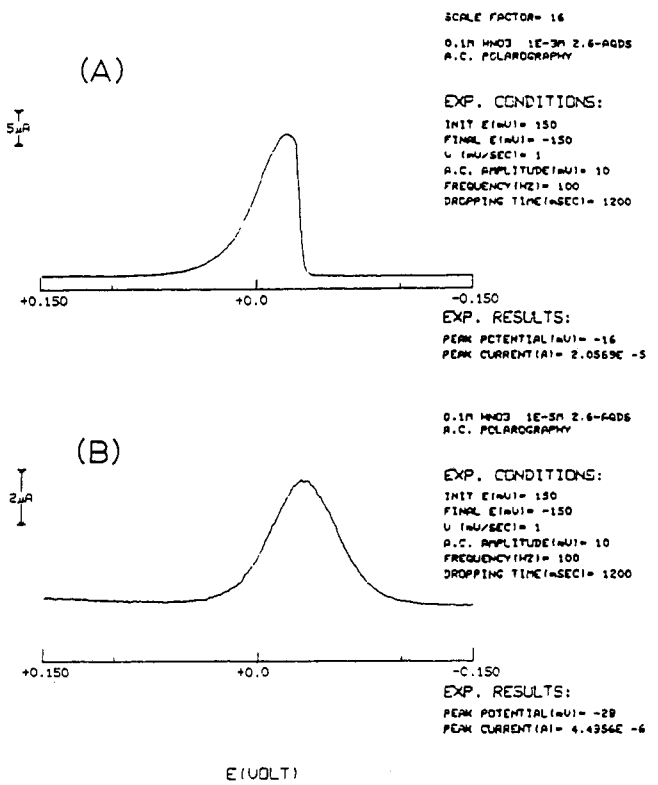

Figure 9. Ac voltammograms of 2,6-AQDS in 0.1 M HNO_3: (A) 1×10^{-3} M 2,6-AQDS, (B) 1×10^{-5} M 2,6-AQDS.

potential corresponding to the spike in the cyclic voltammogram. At potentials more negative than the spike, the oxidized form is reduced and then stabilized, so the activities of both oxidized form and reduced form are very low. Thus, no redox reaction will respond to the ac potential perturbation. As a comparison, an ac voltammogram in 1×10^{-5} M 2,6-AQDS is shown in Figure 9B. There is no spike in the cyclic voltammogram at this low concentration. The ac current response is quite normal, since no reorganization and stabilization of the reduced form seem to happen.

The spike is strongly pH dependent. It vanishes at pH values above 3.5. This phenomenon suggests that there are weaker intermolecular interactions at high pH. The existence and the height of the spike are also dependent on the bulk concentration of 2,6-AQDS. When the bulk concentration is high, the adsorbed species are crowded. The interaction between molecules after reorganization is strong, and the spike height increases with the concentration, but not linearly. When the bulk concentration is lower than 1×10^{-5} M, the surface is not full, and the distance between molecules is large, so the interaction becomes much weaker and the spike disappears.

The molecular basis for reorganization is not very clear. It is evidently due to special, strongly attractive, interactions between reduced 2,6-AQDS, perhaps hydrogen bonding between a hydroxy group on one molecule and a sulfonate group on another. The surface excess charge is positive at potentials between +0.2 and 0.0 V. The aromatic rings of 2,6-AQDS are probably oriented flat, so that both sulfonate groups are bound electrostatically on the electrode–solution interface. However, at a potential a little more positive than 0.0 V, the excess surface charge seems to be sharply reduced, probably as some consequence of the partial reduction of the adlayer. It may abet the reorganization by providing greater freedom of movement for each molecule, or it may be a result of the reorganization. The reduction in surface charge is itself mysterious. It seems explainable by a reorientation of each species from flat-adsorbed to edgewise-adsorbed but only if the layer remains compact, requiring uptake of new adsorbate. Yet there is no change in coverage as the spike develops, even fully. Alternatively, one might explain the result by neutralization of the negative charges on the sulfonate groups, e.g., by protonation.

(28) Laviron, E. *J. Electroanal. Chem.* **1974**, *52*, 355.

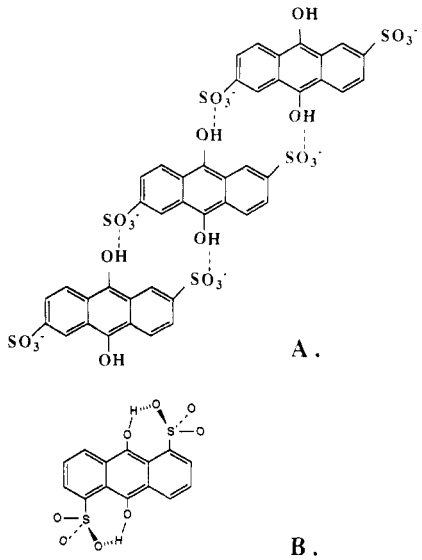

Figure 10. (A) Proposed extended, hydrogen-bonded structure for reduced, adsorbed 2,6-AQDS. (B) Proposed intramolecular hydrogen bonding in 1,5-AQDS.

This view is supported by the pH dependence of the spike, but it is not easy to see why such a sudden change would come about on this basis. Another curious aspect is that the 2,6-AQDS layer seems nearly ideally Langmuirian until the spike starts to emerge at about 1.5×10^{-5} M. This behavior, of course, indicates the absence of lateral interactions; yet the emergence of the spike must be attributed to just such interactions. Since its development is deferred until full coverage is approached, short-range interactions capable of producing, in effect, a phase transition seem to cause it. An attractive possibility is a condensation from a gaslike collection of isolated species into a hydrogen-bonded network like that suggested in Figure 10A. Similar structures are known, for example, in crystals of 2,3-dichloroquinizarin and related compounds.[29] This picture explains many aspects of the system, but not the changes in charge density, at least not in detail. A fuller view must await more experiments.

No sharp spike develops in the 1,5-AQDS system at any coverage. Instead, the voltammetric peaks due to the adsorbate become steadily sharper as the surface coverage increases. At full coverage, the peak width at half-height is only 8 mV. Thus, intermolecular attractions exist even when the surface is far below full.[21,25] The difference in behavior of 1,5-AQDS versus 2,6-AQDS supports a structure-specific model leading only in the latter case to domains of molecules linked by hydrogen bonds. There are inevitable differences between 1,5-AQDS and 2,6-AQDS in their abilities to engage in intermolecular and intramolecular hydrogen bonding. One can imagine a network like that in Figure 10A for 1,5-AQDS, but competing with its development is very likely to be intramolecular hydrogen bonding, like that shown in Figure 10B. Such an intramolecular effect has been reported by Cody[30] for the analogous structure in 8-(phenylamino)naphthalene-1-sulfonate. In reduced 2,6-AQDS, on the other hand, the phenolic protons and the sulfonate group are too far apart to engage in intramolecular hydrogen bonding.

The electrochemical behavior of 1,5-AQDS is in other respects quite different from that of 2,6-AQDS. A cyclic voltammogram for 1,5-AQDS is shown in Figure 11. The diffusive reduction peak occurs at a more negative potential than in Figure 2, and the corresponding reoxidation peak occurs at a more positive potential. Thus, the adlayer seems to slow the kinetics of the couple involving diffusing species to a greater degree than in the case of 2,6-AQDS. Berg[5] noted the difference in kinetics for the 1,5- and 2,6-derivatives and attributed them to the existence of internal hydrogen bonding in the 1,5-AQDS. The differences in

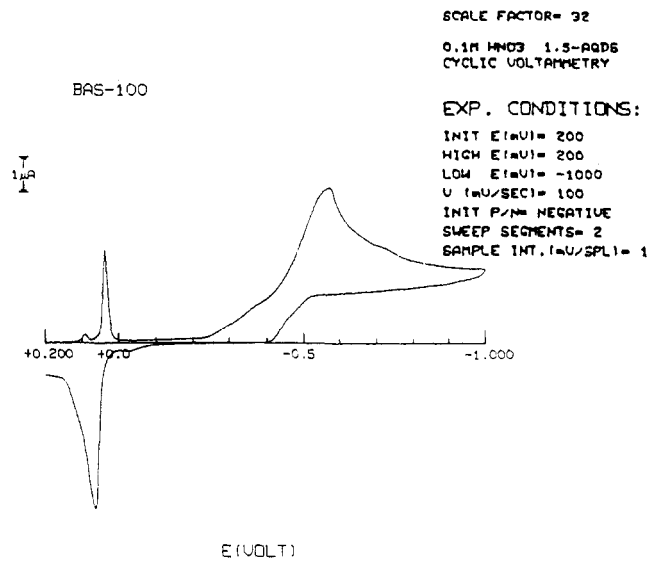

Figure 11. Cyclic voltammogram of 1×10^{-3} M 1,5-AQDS in 0.1 M HNO_3.

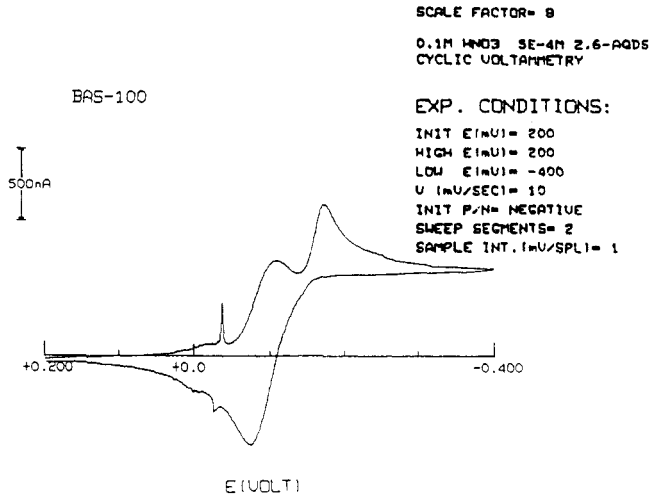

Figure 12. Cyclic voltammogram of 5×10^{-4} M 2,6-AQDS in 0.1 M HNO_3 at 10 mV/s.

the adlayers, whose existence was not realized by Berg, could also cause the difference in reversibility. The reversibility of this electrode reaction descends in the order of 2-AQMS, 2,6-AQDS, and 1,5-AQDS.

Electrocatalysis and Inhibition. The small wave between the adsorption peak and diffusion peak (at −0.1 V in Figure 2) has not been discussed so far. This wave becomes more prominent at low scan rate, as shown in Figure 12. It increases with the bulk concentration but is almost independent of the scan rate when the scan rate is higher than 20 mV/s. If cyclic voltammetry is repeated over many cycles, this peak increases and the diffusion peak decreases. After a few cycles, the middle peak becomes dominant, and the peak separation between the diffusive waves becomes much smaller than on the first cycle. The ease of reduction and oxidation suggests an electrocatalysis of the 2,6-AQDS reaction. However, with still more cycles, the "catalytic" peak decreases, and the main reduction peak becomes very broad and shifts toward more negative potentials, so some sort of inhibition happens. This process is shown in Figure 13. Notice that the spike appears in the first two cycles, and disappears later, after more cycles. Also, the adsorption peak becomes higher and narrower and shifts to more positive potential.

If each potential scan is continued to a more negative limit, in the region where desorption occurs, the growth of the catalytic peak becomes much slower.

The number of cycles needed for catalysis, and then inhibition, depends on the scan rate and bulk concentration, with more cycles

(29) Hall, R. C.; Paul, I. C.; Curtin, D. Y. *J. Am. Chem. Soc.* **1988**, *110*, 2848.
(30) Cody, V. *Biochem. Biophys. Res. Commun.* **1976**, *68*, 425.

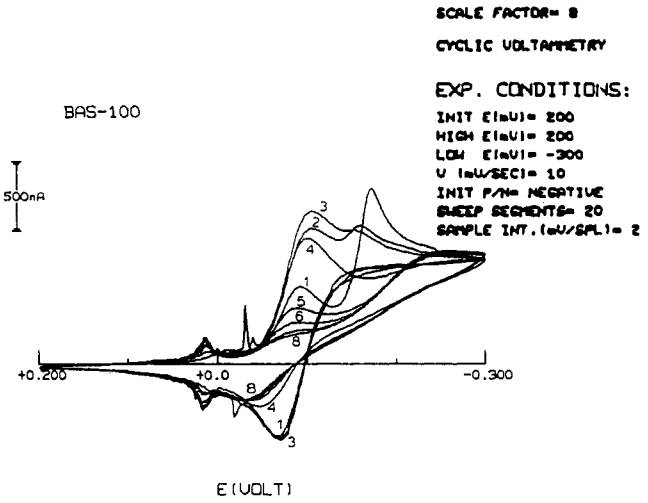

Figure 13. Cyclic voltammograms of 5×10^{-4} M 2,6-AQDS in 0.1 M HNO_3 at 10 mV/s. Successive cycles are numbered in sequence.

being needed at high scan rates or low concentrations. Simply holding the potential somewhere in the adsorption region will cause growth in the catalysis peak in a subsequent cyclic voltammogram.

The origin of the catalysis and inhibition is not clear. It is probably due to the deposition of some kind of extended film (e.g., by precipitation or polymerization) of 2,6-AQDS on the surface of the electrode.[28] In a small quantity, the deposited material may catalyze the reduction and reoxidation of diffusing 2,6-AQDS, but in larger amounts, it may block the reaction, perhaps because of limited electronic conductivity. It is interesting, however, that the reduction of Cd^{2+} is not blocked, even though the reduction potential for Cd^{2+} is still in the adsorption region and the electrode is already sluggish toward the reduction of 2,6-AQDS.

Concluding Remarks. The ease with which 2,6-AQDS and 1,5-AQDS develop very strongly bound, stable, and reversibly active adsorbate layers renders them very attractive for further electrochemical applications. We have, in fact, already begun to use them in studies of fast surface processes at ultramicroelectrodes.[31,32] Additional clarification of fundamental behavior of these substances at interfaces would yield useful scientific insights. High on the agenda should be a fuller exploration of the behavior of 1,5-AQDS and a more secure definition of the chemical basis for the dramatic reorganization in adlayers of 2,6-AQDS.

Acknowledgment. We are grateful to the National Science Foundation for supporting this work through Grants CHE-81-06026 and CHE-86-07984. Ann Zielinski's assistance in the preparation of the final manuscript is greatly appreciated. Professor David Y. Curtin made valuable comments on hydrogen-bonded structures that might exist in our systems.

(31) Faulkner, L. R.; Walsh, M. R.; Xu, C. In *Proceedings of ElectroFinn Analysis, An International Conference on Electroanalytical Chemistry*; Ivaska, A., Ed.; Plenum: New York, in press.
(32) Walsh, M. R.; Xu, C.; Faulkner, L. R. Manuscript in preparation.

Pressure-Induced Coordination Change in the Linear-Chain Metal Halide Complex Trimethylsulfonium Trichloromercurate(II)

A. Brillante,[†,‡] P. Biscarini,[†] and K. Syassen*[,‡]

Dipartimento di Chimica Fisica e Inorganica, Università di Bologna, viale Risorgimento 4, I-40136 Bologna, Italy, and Max-Planck-Institut für Festkörperforschung, Heisenbergstrasse 1, D-7000 Stuttgart 80, Federal Republic of Germany *(Received: June 26, 1989)*

We have measured Raman spectra of the quasi-one-dimensional ionic complex trimethylsulfonium trichloromercurate(II), $[(CH_3)_3S]^+[HgCl_3]^-$, at pressures up to 12 GPa. A major discontinuity in the pressure dependence of intramolecular vibrational frequencies is observed near 1.2 GPa, which is accompanied by drastic changes of band profiles in the Hg–Cl stretching region. An interpretation is given in terms of a pressure-induced stereochemical change, involving an increase of the coordination number of chlorine ligands around the mercury atoms and a change of the anion ($HgCl_3$) local symmetry from planar trigonal to tetrahedral, or pseudotetrahedral. The related stoichiometry involves the presence of either $HgCl_4$ units sharing two apexes along the linear chain or of the dimerized Hg_2Cl_6 species, where one edge is shared between tetrahedral units.

Introduction

The chemistry and spectroscopy of mercury and its coordination compounds have been reviewed in ref 1-3. In this paper we report a high-pressure Raman investigation of trimethylsulfonium trichloromercurate(II), $[(CH_3)_3S]^+[HgCl_3]^-$. This compound (hereafter denoted as $[Me_3S][HgCl_3]$) crystallizes in the monoclinic system, space group $P2_{1/n}$ with $Z = 4$.[4] The crystal structure consists of a trigonal planar arrangement of the $HgCl_3$ moieties. Two additional Hg···Cl contacts contribute to an "effective" coordination number[2] of 5, giving rise to a bridged structure forming quasi-one-dimensional infinite chains, as is illustrated in Figure 1. Each chain is surrounded by sulfonium cations with pyramidal configuration.

The present study aims to investigate whether the above structure could be affected by external pressure via a stereochemical interconversion, going along with a change of the characteristic coordination of mercury. Due to the sensitivity of intramolecular vibrational modes to the metal–halogen coordination, a Raman investigation under pressure of $[Me_3S][HgCl_3]$ can probe structural changes around the metal atom. From the variation of intramolecular Raman-active fundamentals with

[†] Università di Bologna.
[‡] Max-Planck-Institut für Festkörperforschung.

(1) Levason, W.; McAuliffe, C. A. In *The Chemistry of Mercury*; McAuliffe, C. A., Ed.; MacMillan Press: London, 1977; Chapter 2, p 67.
(2) Grdenic, D. *Q. Rev.* **1965**, *19*, 303.
(3) Adams, D. M.; Hills, D. J. *J. Chem. Soc., Dalton Trans.* **1978**, 776, and references therein.
(4) Biscarini, P.; Fusina, L.; Nivellini, G. D.; G. Pelizzi, G. *J. Chem. Soc., Dalton Trans.* **1977**, 664.

0022-3654/90/2094-1141$02.50/0